JOC The Journal of Organic Chemistry

Note

pubs.acs.org/joc

Low Band Gap Coplanar Conjugated Molecules Featuring Dynamic Intramolecular Lewis Acid−Base Coordination

Congzhi Zhu,[†] Zi-Hao Guo,[†] Anthony U. Mu,[†] Yi Liu,[‡] Steven E. Wheeler,[†] and Lei Fang*[,†]

[†]Department of Chemistry, Texas A&M University, 3255 TAMU, College Station, Texas 77843, United States

[‡]The Molecular Foundry, Lawrence Berkeley National Laboratory, One Cyclotron Road, Berkeley, California 94720, United States

Supporting Information

ABSTRACT: Ladder-type conjugated molecules with a low band gap and low LUMO level were synthesized through an N-directed borylation reaction of pyrazine-derived donor−acceptor−donor precursors. The intramolecular boron−nitrogen coordination bonds played a key role in rendering the rigid and coplanar conformation of these molecules and their corresponding electronic structures. Experimental investigation and theoretical simulation revealed the dynamic nature of such coordination, which allowed for active manipulation of the optical properties of these molecules by using competing Lewis basic solvents.

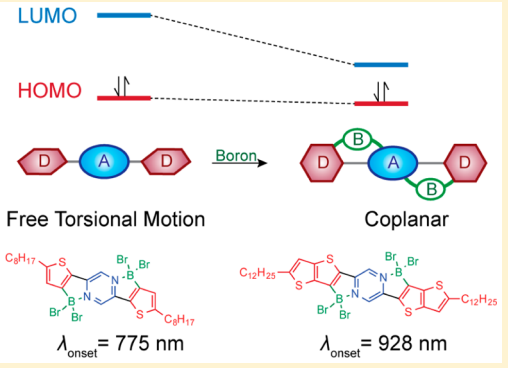

Low band gap materials are pivotally important in applications associated with photovoltaic devices and near-infrared (NIR) absorbing materials.[1−5] Among them, π-conjugated organic materials are particularly captivating on account of their composition of earth-abundant elementals, high photoabsorptivity through direct band gaps, and facile yet controllable solution processability.[6] Two practical strategies are often invoked in the design and synthesis of low band gap π-conjugated organic compounds: (1) Incorporation of conjugated electron-donating and -accepting units in an alternating manner[7−9] and (2) extension of the coherent π-electron delocalization.[10−13]

The first strategy relies on the recombination of the highest occupied molecular orbitals (HOMO) and the lowest unoccupied molecular orbitals (LUMO) of the alternating electron-donating and -accepting units to afford a higher HOMO and a lower LUMO, hence, a narrowed band gap.[14] In order to achieve an extremely low band gap, an electron-rich donor unit is often employed. This approach, however, can lead to the resulting product with a high lying HOMO, which can be easily oxidized and hence suffer from stability issues in an ambient environment.[11] In this context, a more viable strategy for the development of stable low band gap molecules should lower the LUMO level while maintaining the HOMO level. Additionally, lower LUMO energies can lead to *n*-type materials with high electron affinities that are generally less accessible compared to the more widely investigated *p*-type organic materials.[15−17]

In order to apply the second strategy, namely, extension of π-electron delocalization, conjugated polymers are preferable compared to small molecules because of their longer possible conjugation.[18] The effective coherent conjugation length of conventional single-strand polymers, however, is severely limited by the torsional motion in between the aromatic units.[19] A coplanar π-system with restricted torsional disorder, in contrast, is expected to enjoy a much longer coherent conjugation along the backbone.[12,20−25] Thus, locking the entire π-system into a coplanar conformation through a second strand of bonds emerged as an important method toward the development of materials with lower band gaps.[26]

In 2006, Yamaguchi et al. demonstrated[27] the use of noncovalent B−N coordination between a boryl-thienyl unit and an adjacent thiazole unit, which led to a partially coplanar molecule and a lower band gap. Since then, several examples of B−N bond promoted, stepladder-type conjugated small molecules, oligomers, and polymers have been reported.[15,28−38] 38 It is still a challenge, however, to achieve coplanarity of an entirely π-conjugated molecule with more than two aromatic units through B−N bonds. Recently, acceptor−donor−acceptor type conjugated ladder molecules featuring B−N bridging bonds were synthesizied.[30] Analogous donor−acceptor−donor type coplanar molecules, however, have not been achieved yet due to significant deactivation of the nitrogen centers in the central acceptor unit. Herein, we report a new strategy of using B−N coordination to simultaneously achieve (1) coplanarity through the entire π-backbones and (2) low lying LUMO levels in small donor−acceptor−donor molecules. By taking advantage of the dynamic nature of B−N coordination, rational control over the optical activities has been achieved by using competitive Lewis basic solvents. Furthermore, the electronic and optical properties of these molecules featuring dynamic

Received: February 2, 2016
Published: April 20, 2016

DOI: 10.1021/acs.joc.6b00238
J. Org. Chem. 2016, 81, 4347−4352

bonds were studied in detail through a combination of experimental and theoretical tools.

The target model compounds **2** and **4** were designed such that the formation of B−N bonds not only fixes the torsional conformation of the entire π-conjugated system but also strengthens the electron-withdrawing characteristics of the central electron-poor units. The combination of these two effects should lower the LUMO energy levels and band gaps significantly. In these systems, a pyrazine unit was selected as the central electron-accepting unit because it can donate two pairs of electrons in two directions in a central symmetric manner.[34] On the other hand, flanking electron-donating thiophene or thienothiophene units were installed in **2** and **4**, respectively. Because the two nitrogen atoms of the central ring are *para*- to one another, the mutual deactivation effect on their Lewis basicity was relatively weak.[29]

The synthesis of **2** started with Negishi coupling between 2-octylthiophene and dibromopyrazine, which afforded the linear conjugated molecule **1** (Scheme 1). The second step involved *N*-directed electrophilic aromatic substitution of the electron-rich thiophene with BBr_3 (1.0 M solution in CH_2Cl_2).[28,30] Owing to its strong Lewis acidity, BBr_3 was first coordinated with the Lewis basic nitrogen atom on pyrazine. This process made the C_3 position of the thiophene unit spatially favorable for the subsequent electrophilic aromatic substitution. In the presence of diisopropylamine, one-pot formation of two B−N coordination bonds and two C−B covalent bonds was accomplished to construct two stable five-membered rings in the product **2**. These rings fused the two thiophene units and the central pyrazine unit together and confined the conformation of the entire π-system into a coplanar geometry. A similar strategy was adopted to synthesize thienothiophene-derived analogue **4**, which possessed a further extended conjugation backbone with seven fused rings. By treating the precursor **3** with neat BBr_3 as a stronger borylation reagent in the presence of an excess amount of diisopropylamine, **4** was formed and isolated in 53% yield. In either case, the electron-rich nature of the thiophene or thienothiophene promoted the electrophilic substitution reaction in which two C−B covalent bonds and two B−N coordination bonds formed in one pot. ^{11}B NMR spectra corroborated the chemical environment and the sp^3 hybridized nature of the boron center:[37,39−41] the lone pair donated from the nitrogen center shields the boron nuclei, leading to a significant downfield chemical shift on the spectra (Compound **2**: −4.26 ppm; Compound **4**: −4.12 ppm).

Scheme 1. Synthesis of B−N Bridged Donor−Acceptor−Donor Ladder-Type Molecules 2 and 4

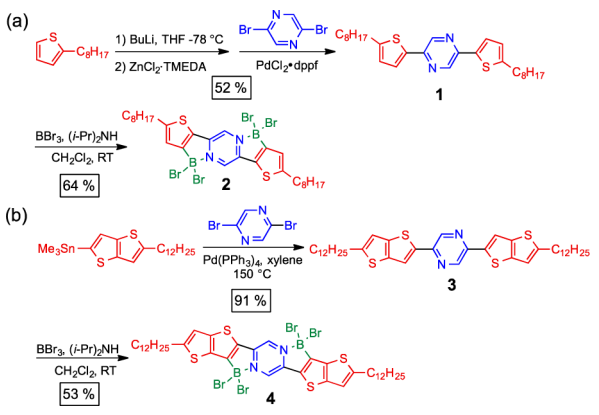

Compared to their precursors **1** and **3**, the absorption spectra of **2** and **4** in $CHCl_3$ ($\sim 9.8 \times 10^{-6}$ M) were dramatically red-shifted to the NIR region (Figure 1), corresponding to low optical band gaps of 1.59 and 1.34 eV, respectively. This drastic red shift can be attributed to planarization effects and the resulting positive overlap between frontier orbitals.[42−44] **4** demonstrated an even lower band gap on account of the extended conjugation and the more electron-rich nature of thienothiophene. Time-dependent density function theory (TD-DFT) was employed to simulate the energy transition and oscillator strength of individual molecules of both **2** and **4** (Figure 1). These computed transitions match well with the experimental spectra. Such good agreement can be attributed to the limited conformational variation in these rigid molecules, thanks to the strong bridging intramolecular B−N bonds. The low energy absorption bands at 700 nm for **2** and at 820 nm for **4** were attributed to the transition from HOMO to LUMO.[45] The transitions from HOMO to LUMO+1 mainly contributed to the absorption below 450 nm with high intensities. The noticeable vibrational progressions presented in the spectra of **2** and **4** in chloroform, even for the low energy HOMO—LUMO bands, further corroborated their rigid conformation in solution.[46,47] In addition, the thin film of **2** demonstrated an almost identical solid-state absorption spectrum compared to that in $CHCl_3$ solution (Figure S7). This observation indicated that there was no significant conformational change from solution phase to solid state, further corroborating the coplanar and rigid backbone of this B−N ladder type molecule.[47]

It is expected that the intrinsically dynamic B−N coordination[48−50] should be controllable in the presence of certain external stimuli. For example, the addition of a Lewis base should weaken this bond by competing for the boron center, shifting the thermodynamic equilibrium toward a less planar conformation. As a result, the electronic structure and optical property of these compounds can be controlled actively: in a Lewis basic solvent, the B−N bond should be more labile and the molecular conformation should be less rigid, leading to a blue-shifted absorption spectrum, and *vice versa*.

In this context, UV−vis−NIR spectra of **2** and **4** were examined in various solvents with varying Lewis basicity. However, it is well-known that solvation effects, such as dipole interaction[51] and electronic polarization,[52,53] can also affect the

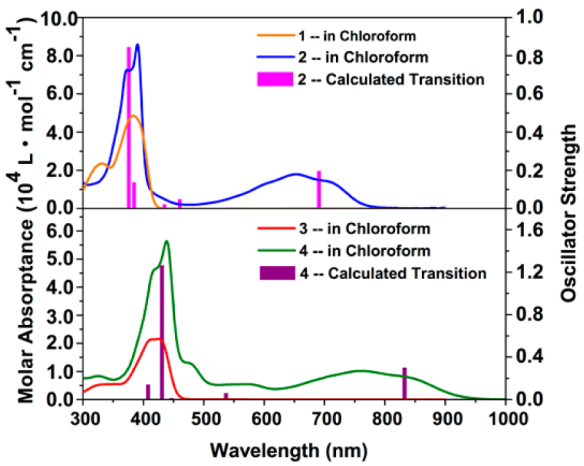

Figure 1. Solution phase UV−vis−NIR spectra and calculated oscillator strength [B3LYP/6-311G(d,p)] of **2** (top) and **4** (bottom), in comparison to their precursor **1** and **3**.

DOI: 10.1021/acs.joc.6b00238
J. Org. Chem. 2016, 81, 4347−4352

absorption and optical band gap. In order to minimize these solvation effects, organic solvents were carefully selected with small and similar dielectric constants (dielectric constants range from 3.8 to 9.2).[54] In general, the low energy absorption peaks were blue-shifted in Lewis basic solvents (Figure 2a, b and Figure S8). The optical HOMO—LUMO band gaps measured in these solvents were plotted against the enthalpies from the complex formation between the solvent and BF_3, which provides a measure of the Lewis basicity of the solvent.[55] The band gap increased monotonically as the Lewis basicity increased (Figure 2c, d), consistent with the weakening of the intramolecular B−N coordination bonds. Moreover, as the Lewis basicity increased, the vibrational progressions gradually disappeared because **2** and **4** were less rigid. Furthermore, to rule out the aforementioned solvation effects, the optical band gaps were also plotted against the dielectric constants of these solvents (Figure S9), showing no significant correlation. To further characterize such Lewis acid−base competition with solvent molecules, variable-temperature NMR analysis of **2** was conducted in weak (CD_2Cl_2) and strong (d_8-THF) Lewis basic solvents, respectively. In d_8-THF, the resonance signal of the central pyrazine proton was found shifted downfield by 0.2 ppm while cooling down from 40 °C to −20 °C (Figure S10), as a result of the more favorable intramolecular B−N coordination interaction and less competitive solvent effect at a lower temperature.[56,57] In contrast, the chemical shift change in CD_2Cl_2 was only 0.06 ppm in this temperature range, because the weaker Lewis base CD_2Cl_2 exerted much weaker solvent competition (Figure S10). Thus, the employment of Lewis basic solvents provides the ability to control the optical band gaps of these dynamic B−N bridged molecules in the NIR region through competitive coordination interactions.

Frontier orbital energy levels of molecules **1**−**4** were investigated by using a combination of experimental and theoretical techniques. Cyclic voltammetry traces (Figure 3a) of **1**−**4** were recorded in solid state after drop-casting the solution of each compound on the working electrode[58] in order to eliminate the impact induced by the Lewis basicity of the electrolyte solution and avoid possible decomposition in solution (Figure S11).[59] Cyclic voltammetry traces of **2** and **4** showed irreversible reduction peaks around −0.4 V versus Fc/Fc^+, which was about 1 V lower than their precursors **1** and **3**, respectively. The oxidation onsets for **1**−**4** were all similar around 0.8 V versus Fc/Fc^+. These values suggested that the B−N bond formation lowered the LUMO level but not the HOMO level, as expected. These experimental data were further corroborated by DFT computations (Figure 3b). Compared to **1** and **3**, both **2** and **4** exhibit dramatically decreased LUMO levels below −4.0 eV, in contrast to the almost unchanged HOMO levels, in agreement with the values from the electrochemical experiments. The coordination between boron and nitrogen significantly lowers the LUMO energy levels for **2** and **4**, with no significant impact on the HOMO levels. As mentioned above, this represents an ideal approach to achieving a low band gap without increasing the HOMO level and reducing stability.

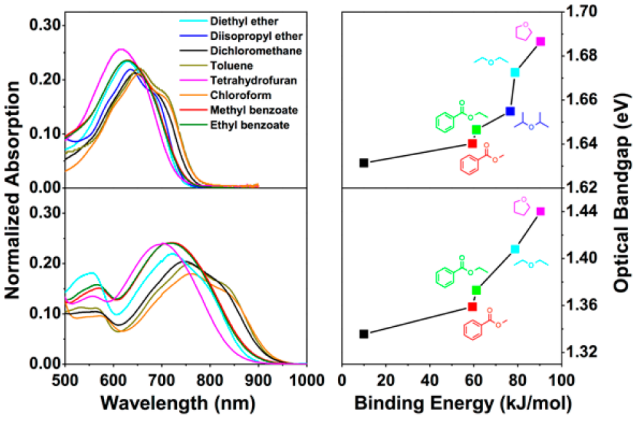

Figure 2. Charge transfer absorption of **2** (a) and **4** (b) in a variety of organic solvents and the correlation between optical band gaps of **2** (c) and **4** (d) with the Lewis basicities of organic solvents (enthalpies from complex formation with BF_3).

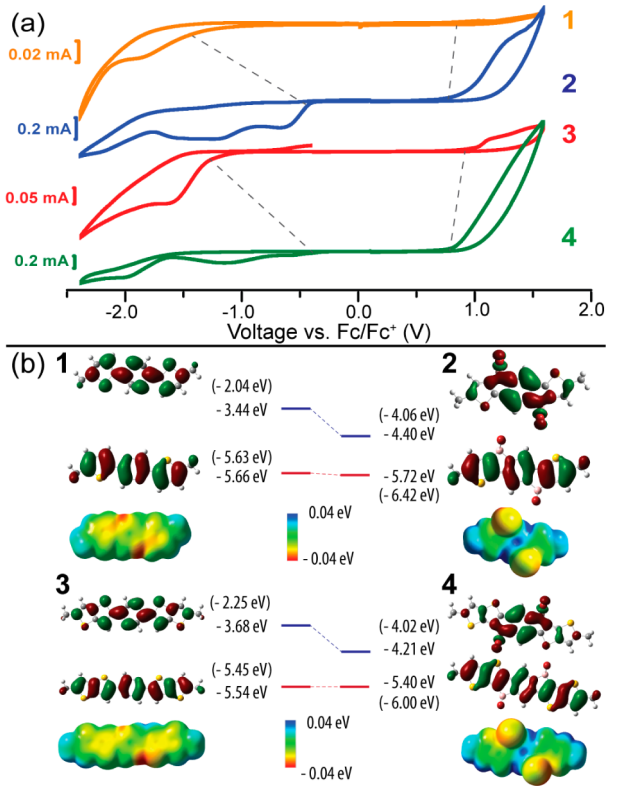

Figure 3. (a) Cyclic voltammetry of **1**−**4**, 0.10 M *n*-Bu_4NPF_6 in CH_3CN, Fc = ferrocene. (The comparison of reduction onsets and oxidation onsets for **2**, **4** and their precursors were shown in dotted lines.) (b) HOMO, LUMO energy levels [experimental data and calculated values (in parentheses)], calculated molecular orbitals, and electrostatic potential map for **1**−**4** [B3LYP/6-311G(d,p)].

In order to understand how the B−N coordination bond impacts the electronic structure and optical activities of **2** and **4**, HOMO, LUMO energy levels and transitions energies were computed for different molecular conformations by changing the dihedral angles between the pyrazine unit and the flanking electron-rich units (see Tables S1 and S2). When the dihedral angles were larger than 40°, the distance between boron and nitrogen (3.15 Å) was too large to form B−N coordination bonds.[4,27,60,61] As a result, the LUMO energy levels were drastically lifted and the calculated band gaps for **2** and **4** and their precursors were increased. Meanwhile, the calculated HOMO—LUMO optical transition was greatly blue-shifted. Furthermore, the distance between boron and nitrogen was manipulated to see the correlation between the coordination bond length and energy levels. As the distance increased, the

DOI: 10.1021/acs.joc.6b00238
J. Org. Chem. 2016, 81, 4347−4352

B−N coordination was weakened, leading to gradually increased LUMO energy levels and wider band gaps (Figure S12). The electrostatic potential maps for **1**−**4** were further computed. As shown in Figure 3b, the electrostatic potential of the thiophene or thienothiophene units increased after the formation of B−N bonds, which is consistent with a depletion of electron density.[35,62−64] The observed upfield shifts of the ^{1}H NMR chemical shifts of the protons of the thiophene or thienothiophene units also provide indirect evidence of this relative depletion of electron density.[65] Additionally, the positive electrostatic potential on pyrazine also increased dramatically after the coordination event, which is again consistent with an increase in partial positive charge. According to the DFT computations, while the HOMOs remain delocalized throughout the molecules, the LUMOs of **2** and **4** were more localized on pyrazine compared to precursors **1** and **3**. This result suggests that the LUMOs of **2** and **4** mainly comprise the π^* orbital of the positively charged pyrazine. Meanwhile, the LUMO + 1 levels of **2** and **4** were still delocalized throughout the molecules, which can be assigned as the π^* orbital of the entire conjugated systems (Figure S13). In other words, the B−N coordination inserted a new energy level (LUMO) between the delocalized π (HOMO) and π^* (LUMO + 1) orbitals of the entire conjugated molecules. Overall, the comprehensive electron-withdrawing effect and the coordination behavior gave rise to the low-lying LUMO levels and the unchanged HOMO levels of **2** and **4**.

In conclusion, an integrated strategy for creating low band gap coplanar organic materials was developed on the basis of intramolecular Lewis acid−base coordination. Facile synthesis of the model compounds was achieved through an *N*-directed borylation reaction on donor−acceptor−donor precursors. The low-lying LUMOs of the resulting small molecules lead to a band gap as low as 1.3 eV. More interestingly, on account of the dynamic nature of the Lewis acid−base coordination, the band gaps of these systems can be actively modulated by external competing reagents, such as Lewis basic solvents. With a low-lying LUMO and coplanar conformation achieved simultaneously, this work provides a promising model for the future design and development of low band gap *n*-type materials.

EXPERIMENTAL SECTION

Starting materials and reagents were purchased from commercial sources and used as received. THF was dried using an IT pure solvent system and used without further treatment. 2-Octylthiophene[66] and (5-dodecylthieno[3,2-*b*]thiophen-2-yl)trimethylstannane[67] were synthesized according to procedures reported in literature. All the reactions were performed under nitrogen and in dry solvents. ^{1}H, ^{13}C NMR spectra were recorded on a 300 or 500 MHz spectrometer, and ^{11}B NMR were recorded on a 400 Hz spectrometer. Variable-temperature NMR spectra were recorded on 500 MHz spectrometers. ^{1}H and ^{13}C chemical shifts were reported in ppm relative to the signals corresponding to the residual nondeuterated solvents ($CDCl_3$: ^{1}H 7.26 ppm, ^{13}C 77.23 ppm). ^{11}B chemical shifts were reported in ppm relative to the signal of $BF_3{\cdot}OEt_2$ (0.00 ppm). High resolution electrospray ionization mass spectra data were obtained via ESI or MALDI mode with a TOF analyzer. UV−vis and UV−vis−NIR absorption sepectra were were performed in a 1.0 cm path-length cuvette, and the neat solvent was used as baseline. Cyclic voltammetry (CV) in the solid state and solution phase was carried out at room temperature in nitrogen-purged acetonitrile and dichloromethane respectively with a CHI voltammetric analyzer. *n*-Bu_4PF_6 (0.1 M) was used as the supporting electrolyte. The conventional three-electrode configuration consists of an ITO (solid state)/glassy carbon (solution phase) working electrode, a platinum wire anxiliary electrode, and a Ag/AgCl electrode with ferrocenium/ferrocene as the standard. Cyclic voltammograms were obtained at a scan rate of 100 mV/s.

2,5-Bis(5-octylthiophen-2-yl)pyrazine (1). 2-Octylthiophene (864 mg, 4.40 mmol) was dissolved in anhydrous THF (4 mL) at −78 °C under nitrogen. BuLi (2.8 mL, 1.6 M in hexane) was added into the solution dropwise over 15 min. The mixture was stirred at −78 °C for 1 h. $ZnCl_2{\cdot}$TMEDA (404 mg, 1.60 mmol) was added into the mixture, and the mixture was warmed up to room temperature slowly over 1 h. A suspension of 2,5-dibromopyrazine (476 mg, 2.00 mmol) and $Pd(dppf)Cl_2{\cdot}CH_2Cl_2$ (0.08 mmol, 65.4 mg) in THF (1.5 mL) was added into the reaction mixture. The resulting mixture was stirred at 50 °C overnight. After being cooled to room temperature, the reaction mixture was washed with 1 M HCl, and EtOAc was added to extract the product. The organic layer was washed with 1 M HCl and H_2O (20 mL × 2). After drying with $MgSO_4$, the organic solution was dried on a rotary evaporator. The product was further purified by column chromatography on SiO_2 [Hexane/CH_2Cl_2 (2:1)]. The product was isolated as a yellow solid (490 mg, yield: 52%). ^{1}H NMR ($CDCl_3$, 300 MHz, 25 °C): δ = 0.88 (t, J = 7.0 Hz, 6H), 1.40−1.25 (m, 20H), 1.72 (m, J = 7.5 Hz, 4H), 2.85 (t, J = 7.5 Hz, 4H), 6.82 (d, J = 4.0 Hz, 2H), 7.46 (d, J = 4 Hz, 2H), 8.77 (s, 2H). ^{13}C NMR ($CDCl_3$, 500 MHz, 25 °C): δ = 14.3, 22.6, 28.9, 29.2, 29.4, 29.7, 31.6, 32.8, 105.2, 125.8, 138.9, 139.2, 146.0, 150.0. HRMS (MALDI-TOF) m/z [M + H]$^+$ Calcd for $C_{28}H_{41}N_2S_2$ 469.2705; Found 469.2728.

4,4,10,10-Tetrabromo-2,8-dioctyl-4,10-dihydro-4λ^4,5λ^4,10λ^4,11λ^4-thieno[3′,2′:3,4][1,2]azoborolo[1,5-*a*]thieno-[3′2′:3,4][1,2]azaborolo[1,5-*d*]pyrazine (2). **1** (188 mg, 0.40 mmol) and *i*-Pr_2NH (0.112 mL, 0.80 mmol) were dissolved in anhydrous CH_2Cl_2 (2 mL) under nitrogen at 0 °C. BBr_3 (2.4 mL, 1 M in CH_2Cl_2) was added into the solution dropwise. After the addition, the reaction mixture was warmed up to room temperature and stirred overnight. The organic solvent was removed under vacuum. The resulting blue solids were washed with H_2O (10 mL × 2) and filtered. After drying, those solids were washed with hexane (10 mL × 3) and dried under vacuum to give the final product as a blue powder (207 mg, yield: 64%). ^{1}H NMR ($CDCl_3$, 500 MHz, 25 °C): δ = 0.89 (t, J = 6.9 Hz, 6H), 1.40−1.30 (m, 20H), 1.77 (m, J = 7.2 Hz, 4H), 2.97 (t, J = 7.5 Hz, 4H), 7.12 (s, 2H), 8.84 (s, 2H). ^{11}B NMR ($CDCl_3$, 128 MHz, 25 °C): −4.26. ^{13}C NMR ($CDCl_3$, 75 MHz, 25 °C): δ = 14.3, 22.9, 29.2, 29.3, 29.4, 30.2, 31.4, 31.6, 127.0, 130.0, 134.9, 143.7, 163.5, 165.2. HRMS (ESI-TOF) m/z [M − H]$^-$ Calcd for $C_{28}H_{37}B_2Br_4N_2S_2$ 806.9295; Found 806.9263.

2,5-Bis(5-dodecylthieno[3,2-*b*]thiophen-2-yl)pyrazine (3). (5-Dodecylthieno[3,2-*b*]thiophen-2-yl)trimethylstannane (729 mg, 1.55 mmol) and 2,5-dibromo-pyrazine (147 mg, 0.62 mmol) were dissolved in anhydrous xylene (5 mL). The solution was degassed, and $Pd(PPh_3)_4$ (89.3 mg, 0.077 mmol) was added. The tube was sealed, and the mixture was stirred at 150 °C for 40 h. After the mixture cooled to room temperature, hexane was added. The dispension was filtered, and the solids were washed with hexane, MeOH, and acetone. After drying under vacuum, the product was isolated as a yellow solid (381 mg, yield: 91%). ^{1}H NMR ($CDCl_3$ and TFA-*d*, 500 MHz, 25 °C): δ = 0.88 (t, J = 7.0 Hz, 6H), 1.40−1.25 (m, 20H), 1.75 (m, J = 7.5 Hz, 4H), 2.93 (t, J = 7.5 Hz, 4H), 7.05 (s, 2H), 8.08 (s, 2H), 9.02 (s, 2H). ^{13}C NMR ($CDCl_3$ and *d*-TFA, 125 MHz, 25 °C): δ = 14.2, 23.0, 29.4, 29.5, 29.6, 29.7, 29.8, 29.9, 31.4, 31.9, 117.1, 123.5, 132.3, 137.0, 140.0, 142.9, 145.4, 157.2. HRMS (ESI-TOF) m/z [M − H]$^-$ Calcd for $C_{40}H_{55}N_2S_4$ 691.3248; Found 691.3288.

7,7,14,14-Tetrabromo-2,9-didodecyl-7,14-dihydro-6λ^4,7λ^4,13λ^4,14λ^4-thieno[2″,3″:4′,5′]thieno[3′,2′:3,4][1,2]-azaborolo[1,5*a*]thieno[2″,3″:4′,5′]thieno[3′,2′:3,4][1,2]-azaborolo[1,5-*d*]pyrazine (4). **3** (67.7 mg, 0.10 mmol) and *i*-Pr_2NH (0.15 mL, 1.27 mmol) were dissolved in anhydrous CH_2Cl_2 (5 mL) under nitrogen at 0 °C. BBr_3 (0.5 mL) was added into the solution dropwise. After the addition, the reaction mixture was warmed up to room temperature and stirred overnight. The organic solvent was removed under vacuum. The resulting green solids were washed with H_2O (10 mL × 2) and filtered. After drying, those solids were washed with hexane (10 mL × 3) and dried under vacuum to give the final product as a deep green powder (54 mg, 53%). ^{1}H NMR ($CDCl_3$, 500

DOI: 10.1021/acs.joc.6b00238
J. Org. Chem. 2016, 81, 4347−4352

MHz, 25 °C): δ = 0.89 (t, J = 6.9 Hz, 6H), 1.20−1.50 (m, 36H), 1.77 (m, J = 7.2 Hz, 4H), 2.97 (t, J = 7.5 Hz, 4H), 7.12 (s, 2H), 8.84 (s, 2H). ^{11}B NMR (CDCl3, 128 MHz, 25 °C): −4.12. ^{13}C NMR ($CDCl_3$, 300 MHz, 25 °C): δ = 14.1, 22.7, 29.1, 29.1, 29.2, 31.2, 31.4, 31.8, 117.4, 131.38, 134.6, 138.7, 144.0, 150.1, 158.6. HRMS (ESI-TOF) m/z $[M - H]^-$ Calcd for $C_{40}H_{53}B_2Br_4N_2S_4$ 1030.9970; Found 1031.0008.

■ ASSOCIATED CONTENT

Supporting Information

The Supporting Information is available free of charge on the ACS Publications website at DOI: 10.1021/acs.joc.6b00238.

^{1}H, ^{13}C NMR spectra of compounds **1** and **3**; ^{1}H, ^{11}B, ^{13}C NMR spectra of compounds **2** and **4**; UV−vis absorption spectra of compounds **2** and **4**; Variable temperature NMR spectra; cyclic voltammetry scans; DFT calculation data (PDF)

■ AUTHOR INFORMATION

Corresponding Author

*E-mail: fang@chem.tamu.edu.

Notes

The authors declare no competing financial interest.

■ ACKNOWLEDGMENTS

We thank Dr. Jodie Lutkenhaus and Dr. Fei Li at TAMU for help with the cyclic voltammetry experiments. Funding is gratefully acknowledged from Texas A&M University and the National Science Foundation (Grant CHE-1254897). Work at the Molecular Foundry was supported by the Office of Science, Office of Basic Energy Sciences, of the U.S. Department of Energy under Contract No. DE-AC02-05CH11231.

■ REFERENCES

(1) Qian, G.; Wang, Z. Y. *Chem. - Asian J.* **2010**, *5*, 1006−1029.
(2) Ajayaghosh, A. *Acc. Chem. Res.* **2005**, *38*, 449−459.
(3) Meier, C.; Gondorf, A.; Lüttjohann, S.; Lorke, A.; Wiggers, H. *J. Appl. Phys.* **2007**, *101*, 103112.
(4) Lu, H.; Mack, J.; Yang, Y.; Shen, Z. *Chem. Soc. Rev.* **2014**, *43*, 4778−4823.
(5) Prabhakar, C.; Yesudas, K.; Krishna Chaitanya, G.; Sitha, S.; Bhanuprakash, K.; Rao, V. J. *J. Phys. Chem. A* **2005**, *109*, 8604−8616.
(6) Gierschner, J.; Cornil, J.; Egelhaaf, H. J. *Adv. Mater.* **2007**, *19*, 173−191.
(7) Müllen, K.; Pisula, W. *J. Am. Chem. Soc.* **2015**, *137*, 9503−9505.
(8) Zhang, Q. T.; Tour, J. M. *J. Am. Chem. Soc.* **1998**, *120*, 5355−5362.
(9) Hwang, B. K.; Gu, Q. M.; Sih, C. J. *J. Am. Chem. Soc.* **1993**, *115*, 7912−7913.
(10) Roncali, J. *Chem. Rev.* **1997**, *97*, 173−206.
(11) Roncali, J. *Macromol. Rapid Commun.* **2007**, *28*, 1761−1775.
(12) Chou, C.-M.; Saito, S.; Yamaguchi, S. *Org. Lett.* **2014**, *16*, 2868−2871.
(13) Cheng, Y.-J.; Yang, S.-H.; Hsu, C.-S. *Chem. Rev.* **2009**, *109*, 5868−5923.
(14) Kim, B.-G.; Ma, X.; Chen, C.; Ie, Y.; Coir, E. W.; Hashemi, H.; Aso, Y.; Green, P. F.; Kieffer, J.; Kim, J. *Adv. Funct. Mater.* **2013**, *23*, 439−445.
(15) Dou, C.; Ding, Z.; Zhang, Z.; Xie, Z.; Liu, J.; Wang, L. *Angew. Chem., Int. Ed.* **2015**, *54*, 3648−3652.
(16) Yan, H.; Chen, Z.; Zheng, Y.; Newman, C.; Quinn, J. R.; Dotz, F.; Kastler, M.; Facchetti, A. *Nature* **2009**, *457*, 679−686.
(17) Ando, S.; Murakami, R.; Nishida, J.-i.; Tada, H.; Inoue, Y.; Tokito, S.; Yamashita, Y. *J. Am. Chem. Soc.* **2005**, *127*, 14996−14997.
(18) Zade, S. S.; Bendikov, M. *Org. Lett.* **2006**, *8*, 5243−5246.
(19) Bjorgaard, J. A.; Köse, M. E. *J. Phys. Chem. A* **2013**, *117*, 3869−3876.
(20) Jin, X.-H.; Sheberla, D.; Shimon, L. J. W.; Bendikov, M. *J. Am. Chem. Soc.* **2014**, *136*, 2592−2601.
(21) Babel, A.; Jenekhe, S. A. *J. Am. Chem. Soc.* **2003**, *125*, 13656−13657.
(22) Uddin, M. A.; Lee, T. H.; Xu, S.; Park, S. Y.; Kim, T.; Song, S.; Nguyen, T. L.; Ko, S.-j.; Hwang, S.; Kim, J. Y.; Woo, H. Y. *Chem. Mater.* **2015**, *27*, 5997−6007.
(23) Wang, X.-Y.; Lin, H.-R.; Lei, T.; Yang, D.-C.; Zhuang, F.-D.; Wang, J.-Y.; Yuan, S.-C.; Pei, J. *Angew. Chem., Int. Ed.* **2013**, *52*, 3117−3120.
(24) Wang, X.-Y.; Zhuang, F.-D.; Wang, R.-B.; Wang, X.-C.; Cao, X.-Y.; Wang, J.-Y.; Pei, J. *J. Am. Chem. Soc.* **2014**, *136*, 3764−3767.
(25) Wang, X.-Y.; Wang, J.-Y.; Pei, J. *Chem. - Eur. J.* **2015**, *21*, 3528−3539.
(26) Tsuda, A.; Osuka, A. *Science* **2001**, *293*, 79−82.
(27) Wakamiya, A.; Taniguchi, T.; Yamaguchi, S. *Angew. Chem., Int. Ed.* **2006**, *45*, 3170−3173.
(28) Ishida, N.; Moriya, T.; Goya, T.; Murakami, M. *J. Org. Chem.* **2010**, *75*, 8709−8712.
(29) Agou, T.; Kobayashi, J.; Kawashima, T. *Chem. - Eur. J.* **2007**, *13*, 8051−8060.
(30) Crossley, D. L.; Cade, I. A.; Clark, E. R.; Escande, A.; Humphries, M. J.; King, S. M.; Vitorica-Yrezabal, I.; Ingleson, M. J.; Turner, M. L. *Chem. Sci.* **2015**, *6*, 5144−5151.
(31) Hudson, Z. M.; Ko, S.-B.; Yamaguchi, S.; Wang, S. *Org. Lett.* **2012**, *14*, 5610−5613.
(32) Li, D.; Zhang, H.; Wang, Y. *Chem. Soc. Rev.* **2013**, *42*, 8416−8433.
(33) Dou, C.; Long, X.; Ding, Z.; Xie, Z.; Liu, J.; Wang, L. *Angew. Chem., Int. Ed.* **2016**, *55*, 1436−40.
(34) Hao, Q.; Yu, S.; Li, S.; Chen, J.; Zeng, Y.; Yu, T.; Yang, G.; Li, Y. *J. Org. Chem.* **2014**, *79*, 459−464.
(35) Sengupta, A.; Doshi, A.; Jäkle, F.; Peetz, R. M. *J. Polym. Sci., Part A: Polym. Chem.* **2015**, *53*, 1707−1718.
(36) Crossley, D. L.; Cid, J.; Curless, L. D.; Turner, M. L.; Ingleson, M. J. *Organometallics* **2015**, *34*, 5767−5774.
(37) Wakamiya, A.; Murakami, T.; Yamaguchi, S. *Chem. Sci.* **2013**, *4*, 1002−1007.
(38) Wakamiya, A.; Yamaguchi, S. *Bull. Chem. Soc. Jpn.* **2015**, *88*, 1357−1377.
(39) Hermanek, S. *Chem. Rev.* **1992**, *92*, 325−362.
(40) Cui, C.; Bonder, E. M.; Jäkle, F. *J. Am. Chem. Soc.* **2010**, *132*, 1810−1812.
(41) Ledoux, A.; Larini, P.; Boisson, C.; Monteil, V.; Raynaud, J.; Lacôte, E. *Angew. Chem., Int. Ed.* **2015**, *54*, 15744−15749.
(42) Prabhakar, C.; Chaitanya, G. K.; Sitha, S.; Bhanuprakash, K.; Rao, V. J. *J. Phys. Chem. A* **2005**, *109*, 2614−2622.
(43) Yesudas, K.; Chaitanya, G. K.; Prabhakar, C.; Bhanuprakash, K.; Rao, V. J. *J. Phys. Chem. A* **2006**, *110*, 11717−11729.
(44) Srinivas, K.; Prabhakar, C.; Devi, C. L.; Yesudas, K.; Bhanuprakash, K.; Rao, V. J. *J. Phys. Chem. A* **2007**, *111*, 3378−3386.
(45) Considering the low concentration of the solution samples and the good agreement between TD-DFT calculation and experiment, such a significant red shift of the absorption was attributed to the intrinsic narrower band gaps of the individual molecules rather than an aggregation effect.
(46) He, B.; Dai, J.; Zherebetskyy, D.; Chen, T. L.; Zhang, B. A.; Teat, S. J.; Zhang, Q.; Wang, L.; Liu, Y. *Chem. Sci.* **2015**, *6*, 3180−3186.
(47) Lee, J.; Rajeeva, B. B.; Yuan, T.; Guo, Z.-H.; Lin, Y.-H.; Al-Hashimi, M.; Zheng, Y.; Fang, L. *Chem. Sci.* **2016**, *7*, 881−889.
(48) Steciuk, I.; Durka, K.; Gontarczyk, K.; Dabrowski, M.; Lulinski, S.; Wozniak, K. *Dalton Trans.* **2015**, *44*, 16534−16546.
(49) Luisier, N.; Scopelliti, R.; Severin, K. *Soft Matter* **2016**, *12*, 588−593.
(50) Chen, J.; Lalancette, R. A.; Jäkle, F. *Chem. - Eur. J.* **2014**, *20*, 9120−9129.

DOI: 10.1021/acs.joc.6b00238
J. Org. Chem. 2016, 81, 4347−4352

(51) McRae, E. G. *J. Phys. Chem.* **1957**, *61*, 562−572.
(52) Limantara, L.; Sakamoto, S.; Koyama, Y.; Nagae, H. *Photochem. Photobiol.* **1997**, *65*, 330−337.
(53) Lee, F. S.; Chu, Z. T.; Warshel, A. *J. Comput. Chem.* **1993**, *14*, 161−185.
(54) Strong Lewis basic solvents such as DMF, acetonitrile, and pyridine are excluded in this study because they have very large dielectric constants (DMF, 38.3; acetonitrile, 36.6; pyridine, 12.3). Data source: American Chemical Society (https://www.organicdivision.org/orig/organic_solvents.html). Fluride reagents were also excluded because **2** and **4** decomposed in solution upon the addition of TBAF and KF.
(55) Maria, P. C.; Gal, J. F. *J. Phys. Chem.* **1985**, *89*, 1296−1304.
(56) Gellman, S. H.; Dado, G. P.; Liang, G. B.; Adams, B. R. *J. Am. Chem. Soc.* **1991**, *113*, 1164−1173.
(57) Lämmermann, A.; Szatmári, I.; Fülöp, F.; Kleinpeter, E. *J. Phys. Chem. A* **2009**, *113*, 6197−6205.
(58) Guo, Z.-H.; Ai, N.; McBroom, C. R.; Yuan, T.; Lin, Y.-H.; Roders, M.; Zhu, C.; Ayzner, A. L.; Pei, J.; Fang, L. *Polym. Chem.* **2016**, *7*, 648−655.
(59) Compounds **2** and **4** showed good stability toward water in solids, but they can decompose slowly in solution when exposed to water (Figure S5).
(60) Icli, B.; Sheepwash, E.; Riis-Johannessen, T.; Schenk, K.; Filinchuk, Y.; Scopelliti, R.; Severin, K. *Chem. Sci.* **2011**, *2*, 1719−1721.
(61) Wang, L.; Wang, K.; Zhang, H.; Jiao, C.; Zou, B.; Ye, K.; Zhang, H.; Wang, Y. *Chem. Commun.* **2015**, *51*, 7701−7704.
(62) Wheeler, S. E. *J. Am. Chem. Soc.* **2011**, *133*, 10262−10274.
(63) Wheeler, S. E.; Bloom, J. W. G. *Chem. Commun.* **2014**, *50*, 11118−11121.
(64) Wheeler, S. E. *Acc. Chem. Res.* **2013**, *46*, 1029−1038.
(65) Yin, X.; Chen, J.; Lalancette, R. A.; Marder, T. B.; Jäkle, F. *Angew. Chem., Int. Ed.* **2014**, *53*, 9761−9765.
(66) Geese, K.; Prehm, M.; Tschierske, C. *J. Mater. Chem.* **2010**, *20*, 9658−9665.
(67) Chen, L.; Baumgarten, M.; Guo, X.; Li, M.; Marszalek, T.; Alsewailem, F. D.; Pisula, W.; Müllen, K. *J. Mater. Chem. C* **2014**, *2*, 3625−3630.

DOI: 10.1021/acs.joc.6b00238
J. Org. Chem. 2016, 81, 4347−4352